

INTERNATIONAL JOURNAL OF

ADVANCED ROBOTIC SYSTEMS

volume 8 | number 5 | 2011 | ISSN 1729-8806



INTECH
open science | open minds

International Journal of Advanced Robotic Systems
Volume 8, Number 5, 2011

Abstracted/Indexed in

ISI Thomson Science Citation Index Expanded, Cambridge Scientific Abstracts, Compendex, Current Contents, INSPEC, Recent Advances in Manufacturing, Scopus, Ulrich's Periodical Directory, Scirus, WorldCat, BASE, DOAJ, NSK

Published by InTech

Janeza Trdine 9, 51000 Rijeka, Croatia

Identification Statement

ISSN 1729-8806

Abbreviated key title: Int J Adv Robotic Sy

Start year: 2004

Copyright © 2010 InTech

All articles are Open Access distributed under the Creative Commons Attribution 3.0 license, which permits to copy, distribute, transmit, and adapt the work in any medium, so long as the original work is properly cited. After this work has been published by InTech, authors have the right to republish it, in whole or part, in any publication of which they are the author, and to make other personal use of the work. Any republication, referencing or personal use of the work must explicitly identify the original source.

As for readers, this license allows users to download, copy and build upon published articles even for commercial purposes, as long as the author and publisher are properly credited, which ensures maximum dissemination and a wider impact of our publications.

Notice

Statements and opinions expressed in the articles are these of the individual contributors and not necessarily those of the editors or publisher. No responsibility is accepted for the accuracy of information contained in the published articles. The publisher assumes no responsibility for any damage or injury to persons or property arising out of the use of any materials, instructions, methods or ideas contained in the journal.

Cover Image Copyright 2006. Used under license from Shutterstock.com

Postmaster Send address corrections to ars@intechweb.org or InTech, Janeza Trdine 9, 51000, Rijeka

Determination of An Optimal Return-path on Road Attributes for Mobile Robot Recharging

Regular Paper

Fei Liu, Shan Liang* and Xiaodong Xian

College of Automation, Chongqing University, China

* Corresponding author E-mail: lightsun@cqu.edu.cn

Received 26 July 2011; Accepted 14 October 2011

© 2011 Liu et al.; licensee InTech. This is an open access article distributed under the terms of the Creative Commons Attribution License (<http://creativecommons.org/licenses/by/2.0>), which permits unrestricted use, distribution, and reproduction in any medium, provided the original work is properly cited.

Abstract Optimal path-planning for mobile robot recharging is a very vital requirement in real applications. This paper proposes a strategy of determining an optimal return-path in consideration of road attributes which include length, surface roughness, road grade and the setting of speed-control hump. The road in the environment is partitioned into multiple segments, and for each one, a model of cost that the robot will pay for is established under the constraints of the attributes. The cost consists of energy consumption and the influence of vibration on mobile robot that is induced by motion. The return-path is constituted by multiple segments and its cost is defined to be the sum of the cost of each segment. The idle time, deduced from the cost, is firstly used as the decision factor for determining the optimal return-path. Finally, the simulation is given and the results prove the effectiveness and superiority of the strategy.

Keywords Mobile robot recharging, Road attribute, Surface roughness, Road grade, Idle time.

1. Introduction

Autonomous mobile robots have been developed to perform numerous routine tasks, such as automatic patrolling in a transformer substation [1], transporting in a warehouse [2] and guiding working in a museum [3]. Each application desires the autonomous mobile robots smart enough to survive in its environment without operator intervention. Energy is of crucial concern, and without it the robot will become immobilized and useless [4, 5]. Typically, rechargeable batteries may only provide a few hours of peak usage for the robot once, for example, with a battery pack, a Honda humanoid robot can run for only 30 mins [6]. As a result, to achieve true long-term autonomy, the robot must find a charging station and recharge itself before the power of the batteries is exhausted [7]. Therefore, the important issue of optimal path planning on energy-minimizing attracts considerable attentions continuously.

In indoor environment or square of fine surface, usually the amount of energy consumption is approximately proportional to the length of path that the robot has passed. Hence, for simplicity, some researchers plan to

search the shortest obstacle-avoiding paths, which are recognized as the optimal paths [8–12]. However, in outdoor environments, the criterion of the shortest-length may no longer be suitable because motion of the robots is highly influenced by terrain characteristics [13, 14]. There are few existing methods for field robot navigation that consider this restraint and other criterions such as minimum-time and minimum energy cost are adopted [15–19]. In [18], a number of constraints such as impermissible traversal directions are employed since the environment aimed at is the huge wild area (e.g., a river basin referred in the article). It is thus inevitable to cause the complexity of computing. In the studies on minimum weighted paths planning [15, 16, 19], the weight (e.g., the cost of time or energy consumption) is used as a parameter for theoretical analysis, but no detail of the derivation of the relation between the weight and the road attributes is involved. Additionally, the problem of minimum-time path planning in a 2-1/2-D environment is investigated [17]. However, the assumption is that the robot is working with maximum power, and then time is used as the decision factor for optimal path determination. It is worth mentioning that, Guo et al. adopt the terrain roughness and terrain slope to define the power consumption. However, although it has qualitative analysis, no experiment is executed for quantitative analysis [20]. Besides, Mei et al. discuss the most energy-efficient path planning [13]. However, it focuses on the discussion about energy spent on robot's turning and rotating, while the terrain characteristics are not mentioned.

Furthermore, the dynamic and kinematic constraints are also considered in motion plan. For example, for arbitrarily contoured terrain such as hilly terrain, the anisotropic friction, gravity effects and ranges of impermissible-traversal headings are discussed for overturn danger or power limitation [21]. The dynamic and wheel/ground interaction constraints are dealt with in the motion planning for all-terrain robots, where the environment is thought to be composed of a set of static obstacles, sticky areas and slippery regions [22]. In [20], Guo et al. propose path planning and control of nonholonomic mobile robots in rough terrain environments, where performance issues including robot safety, geometric, time-based and physics-based criteria are refereed. In addition, Kobilarov et al. present a planner that finds near optimal trajectories on outdoor terrain based on control-driven probabilistic road maps [23]. They consider the safety of the robot and use an upper bound on the maximum pitch of the robot. All these indicate that the influence of motion on robot should not be neglected in outdoor environment. Nevertheless, in the majority of the studies currently presented in the literature, the terrain characteristics are just considered as constraints for various purposes in

path planning, but without quantitative analysis. Moreover, researches have tried to classify the terrain based on vibrations induced by wheel-terrain interaction [24, 25]. Different terrain surfaces have different influence on robot, but the authors did not show the impact on the robot in practical application.

As the improvement and synthesis, in our approach of determining the optimal return-path, we take into account both energy consumption and the quantitative analysis on the influence of vibration on mobile robot. Generally, once energy consumption occurs, the robot will spend some time on recharging to compensate the loss, and the time here, is called the idle time which means non-working time. Similarly, the time spent on repairing the robot belongs to the idle time too. Usually, it might take several hours or more to check and repair once the robot is found in abnormal operation state. The reason for repairing is mainly the continuous vibration which may loose the connections among equipments of the robot. And the vibration will exist as long as the robot is walking. Naturally, if the total idle time is minimized, then the working time will be maximized. Hence, we plan to determine an optimal return-path with minimum idle time. To our knowledge, it is the first time to use idle time as the decision factor, which is proved to be more effective for evaluating paths.

This paper is organized as follows: this section has summarized related work and proposed our strategy. In Sect. 2 the research problem and motivation are stated. In Sect. 3 the models of working environment and road attributes are described. In Sect. 4 we address the implementation of the strategy proposed. In Sect. 5 simulation and results are provided as well as discussions. Finally, conclusion is made and further study is announced.

2. Problem Statement and Motivation

In outdoor environment, some special scenarios should be emphasized, e.g., the situations shown in Fig. 1.

In Fig. 1(a), a robot is walking on a path having plain surface while in Fig. 1(b), it is walking on a road of rough surface. In Fig. 1(c) the robot is going straight downhill on a slope and in Fig. 1(d) it is passing a speed-control hump. These reveal the diverse situations in outdoor environment. Because of these various features, the following phenomena will inevitably occur: (i) the bad influence of vibration on equipments is bigger when the robot runs on a rough road compared to a plain one, and more energy consumption rate is destined since of the bigger surface resistance [26]; (ii) on the same slope, different energy consumption rates occur since the robot may be going uphill or downhill; (iii) drastic vibration

occurs while the robot is passing over a speed-control hump compared to walking on ordinary road surface. As a result, the same road or different roads with the same length may cost different energy consumption and have influences of different level on the robot's body.

The analysis above shows that path length will no longer be suitable for evaluating the paths in outdoor environment, since extra energy consumption rate and influence of vibration on robot exist. As mentioned in Sect. 1, this paper endeavors to determine the optimal path using the idle time as the decision factor. From a different angle, we say that less idle time means the prolonged working-time. This conforms to the target that maximizing the rate of working. Hence, the main task is to clarify how the road attributes are employed to analyze the impact on idle time.

In this paper, the road in the environment is divided into multiple segments, whose attributes can be pre-collected. We first find out each path accessible to a certain dock, and compute the cost by summing the costs of the multiple road segments consisting this path. The optimal return-path with minimum idle time will be selected out. Therefore, in this paper, great efforts are made to deduce the quantitative relation between the idle time and the multiple attributes of road.

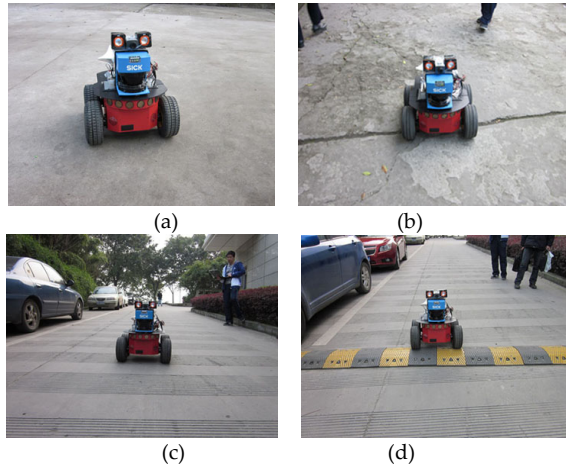


Figure 1. Four typical situations in practice: a robot is (a) walking on a flat road; (b) walking on a rough road; (c) walking on a slope and (d) passing a speed-control hump.

3. The Model of Working Environment

This section establishes the model of working environment by using a metric topological map. First, some assumptions are made:

(a). There has H docks placed in the environment, which are noted as $D_0, D_1, \dots, D_h, \dots, D_{H-1}$ respectively. For example, in Fig. 2, D_h is a dock.

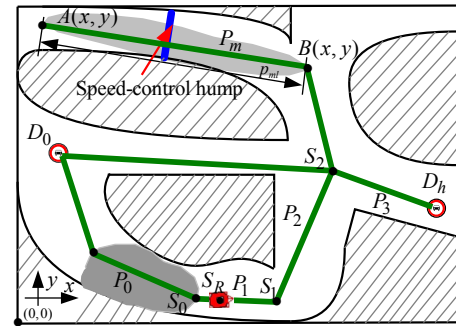


Figure 2. The model of working environment. D_h is a dock, P_m shown as a green line is a road segment. Each blue line represents a speed-control hump. The shadow implies that it is a rough segment. The regions with oblique lines represent obstacles.

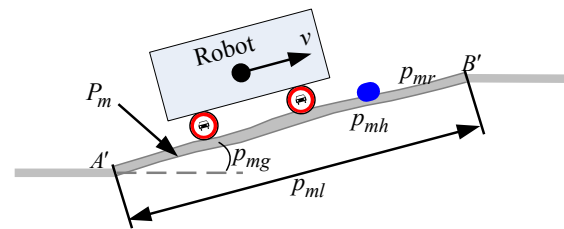


Figure 3. The attributes p_{ml} , p_{mr} , p_{mg} and p_{mh} of a segment P_m .

(b). The road is partitioned into M segments. Each segment P_m ($m = 0, 1, \dots, M-1$) has four attributes: p_{ml} , p_{mr} , p_{mg} and p_{mh} , where p_{ml} (unit: m) represents the length of P_m , p_{ml} (unit: m/km) is the surface roughness, and p_{mh} implies how many speed-control humps are fixed on this segment. p_{mg} (unit: rad) is the actual road grade of P_m , and $-\pi/2 < p_{mg} < \pi/2$. The four properties can be understood more clearly by the profile of a segment shown in Fig. 3.

Specifically, the sign of p_{mg} is decided by the coordinates of the two endpoints. In the coordinate system shown in Fig. 2, for P_m , $A(x, y)$ represents one endpoint that has smaller abscissa value or smaller ordinate value and the same abscissa value with the other endpoint. We note the other point as $B(x, y)$. According to Fig. 3, for P_m in Fig. 2, the sign of p_{mg} is decided by

$$\begin{cases} p_{mg} \geq 0, & A(x, y) \text{ corresponds to } A' \text{ actually} \\ p_{mg} < 0, & A(x, y) \text{ corresponds to } B' \text{ actually} \end{cases} \quad (1)$$

Observed from (1), if $p_{mg} > 0$, the robot is uphill actually when going from A to B or else downhill.

(c). The cost that the robot will pay for passing each segment includes two parts: energy consumption c_e and

the influence of vibration on robot body c_b that describes the probability of robot's equipment failure. The cost C then can be described as

$$C = (c_e, c_b) \quad (2)$$

4. The Implementation of the Strategy

In this section, the force analysis when the robot is walking on a road segment is carried out first, then the mathematical models of c_e and c_b are established based on the road attributes. At last the strategy of determining the optimal return-path is described in detail using c_e and c_b .

4.1 The Force Analysis of the Mobile Robot

A longitudinal robot model is built to analyze the forces shown in Fig. 4. The robot is constrained by five forces: the engine force F_{engine} , the rolling resistance F_{roll} , the brake force F_{brake} , the air drag F_{air} and the gravity induced force $F_{gravity}$ respectively [27].

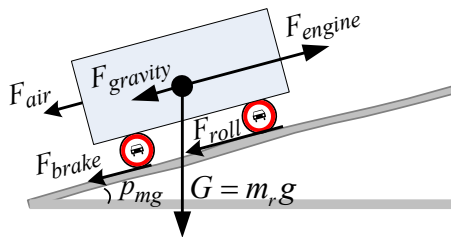


Figure 4. Force analysis of the mobile robot when passing a road segment.

Given a robot walking at low speed and without braking, the impact of F_{air} and F_{brake} are omitted, then we obtain

$$\begin{cases} F_{air} = 0 \\ F_{brake} = 0 \end{cases} \quad (3)$$

With Fig. 4, F_{roll} can be expressed as

$$F_{roll} = \gamma_r m_r g \cos(p_{mg}) \quad (4)$$

where γ_r is the coefficient of rolling resistance that is proportional to p_{mr} . Let $\rho (\rho > 0)$ be the proportion, i.e., $\gamma_r = \rho p_{mr}$, then

$$F_{roll} = \rho p_{mr} m_r g \cos(p_{mg}) \quad (5)$$

In addition, $F_{gravity}$ is induced by gravity G , and the relation between $F_{gravity}$ and p_{mg} is

$$F_{gravity} = m_r g \sin(p_{mg}) \quad (6)$$

where m_r is the weight of the robot and g is the gravitational constant.

Assume that the robot walks at a constant velocity, that is to say, the acceleration is zero, and then with (3) we obtain

$$F_{engine} = F_{roll} + F_{gravity} \quad (7)$$

4.2 Computation of the Idle Time

This section will first deduce the mathematical models of c_e and c_b according to the attributes and force analysis above, and then based upon the models we compute the idle time.

4.2.1 Mathematical Model of c_e

Define $W_{p_{ml}}$ as the total work the robot does when moving for distance p_{ml} dragged by F_{engine} , and assume no energy consumption for making turns, then

$$W_{p_{ml}} = F_{engine} p_{ml} \quad (8)$$

According to (5), (6) and (7) additionally, we have

$$W_{p_{ml}} = \rho p_{mr} m_r g \cos(p_{mg}) p_{ml} + m_r g \sin(p_{mg}) p_{ml} \quad (9)$$

In this paper, the energy the robot needs to drive motors is supplied by batteries. We assume the energy consumption is proportional to the total work, i.e., $c_e \propto W_{p_{ml}}$. Thus, we describe c_e using $W_{p_{ml}}$ and a positive coefficient λ as

$$c_e = \lambda W_{p_{ml}} \quad (10)$$

As c_e is the result of long-term accumulation of energy consumption, the energy spent on passing a single speed-control hump can be ignored. We define r_e (unit: V/m) as the energy consumption rate of walking on road, which means the average voltage decrease (unit: V) of passing per meter long road. Therefore, for passing a road segment P_m with attribute p_{ml} , c_e is calculated as

$$c_e = r_e p_{ml} \quad (11)$$

According to (9), (10) and (11), we get

$$r_e = \rho p_{mr} \lambda m_r g \cos(p_{mg}) + \lambda m_r g \sin(p_{mg}) \quad (12)$$

Let $\kappa = \lambda m_r g$, then (12) becomes

$$r_e = \kappa \rho p_{mr} \cos(p_{mg}) + \kappa \sin(p_{mg}) \quad (13)$$

We will discuss two situations in terms of p_{mg} and p_{mr} :

(a). $p_{mg} = 0$ and $p_{mr} = \mu_f$.

First, we consider that a road has attributes $p_{mg} = 0$ and $p_{mr} = \mu_f$. According to (13), we obtain the energy consumption rate $r_{e_ \mu_f}$ of this situation:

$$r_{e_ \mu_f} = \kappa \rho \mu_f \quad (14)$$

Define $r_{e_ p_{mr}}$ as the energy consumption rate for passing any segment of $p_{mg} = 0$ and p_{mr} , then with (14) we have

$$r_{e_ p_{mr}} = \kappa \rho p_{mr} = \frac{p_{mr}}{\mu_f} r_{e_ \mu_f} \quad (15)$$

(b). $p_{mg} = \varphi_g (\varphi_g \neq 0)$ and $p_{mr} = \mu_f$.

Define $r_{e_ \mu_f \varphi_g}$ as the energy consumption for a segment having attributes $p_{mg} = \varphi_g$ and $p_{mr} = \mu_f$, then with (13) we have

$$r_{e_ \mu_f \varphi_g} = \kappa \rho \mu_f \cos \varphi_g + \kappa \sin \varphi_g \quad (16)$$

then with (14) and (16), we have

$$\kappa \sin \varphi_g = r_{e_ \mu_f \varphi_g} - r_{e_ \mu_f} \cos \varphi_g \quad (17)$$

According to (13) - (17), for any segment having attributes p_{mg} and p_{mr} , we have

$$r_e = \frac{r_{e_ \mu_f}}{\mu_f} p_{mr} \cos(p_{mg}) + \frac{r_{e_ \mu_f \varphi_g} - r_{e_ \mu_f} \cos \varphi_g}{\sin(\varphi_g)} \sin(p_{mg}) \quad (18)$$

With given values μ_f and φ_g , if $r_{e_ \mu_f}$ and $r_{e_ \mu_f \varphi_g}$ are measured experimentally, the energy consumption rate r_e for passing any segment P_m of attributes p_{mg} and p_{mr} can be obtained.

$$\text{Let } \Delta r_{e_ r} = \frac{r_{e_ \mu_f}}{\mu_f} \text{ and } \Delta r_{e_ g} = \frac{r_{e_ \mu_f \varphi_g} - r_{e_ \mu_f} \cos \varphi_g}{\sin(\varphi_g)}, \quad (18)$$

Becomes

$$r_e = \Delta r_{e_ r} p_{mr} \cos(p_{mg}) + \Delta r_{e_ g} \sin(p_{mg}) \quad (19)$$

With (11) and (19), the energy consumption c_e of passing P_m is obtained

$$c_e = (\Delta r_{e_ r} p_{mr} \cos(p_{mg}) + \Delta r_{e_ g} \sin(p_{mg})) p_{ml} \quad (20)$$

4.2.2 Mathematical Model of c_b

The vibration on robot is caused by lots of factors such as the nonlinearity of robot body, speed-control hump and the road surface roughness [26]. Here, we mainly focus on the latter two factors. Define $c_{b_ r}$ as the influence caused by passing road surface and $r_{b_ r}$ as the average influence of passing per meter long road, then

$$c_{b_ r} = r_{b_ r} p_{ml} \quad (21)$$

A system's reliability is usually indicated by the Mean Time Between Failures (MTBF). Here, we define the Mean Length Between Maintenances (MLBM) in a similar way to describe the quality of connections among devices in the robot. Here, MLBM implies the average length of path the robot has traveled between two successive maintenances. Hence, the practical meaning of $r_{b_ r}$ is the average probability value leading the robot to be repaired when the robot passes per meter long road with certain speed. We use L_{MLBM} (unit: m) to express the value of MLBM. Assume that L_{MLBM} is measured to be $L m$, i.e., $L_{MLBM} = L m$, then we obtain

$$r_{b_ r} = \frac{1}{L_{MLBM}} = \frac{1}{L} m^{-1} \quad (22)$$

If the average influence is measured to be $r_{b_ \mu_f}$ for P_m of given surface roughness $p_{mr} = \mu_f$, then

$$r_{b_ r} = \frac{p_{mr}}{\mu_f} \eta r_{b_ \mu_f} \quad (23)$$

where $\eta (\eta > 0)$ implicates the proportional relation between the influence degree and surface roughness.

For a slope, the extra influence caused by road grade is ignored since no extra vibration will occur compared with a road whose road grade is zero. Hence we set the extra influence of slope $r_{b_ s}$ to be zero, i.e., $r_{b_ s} = 0$.

The speed-control humps will bring about vertical vibration with much bigger amplitude compared to road surface. Define $r_{b_ h}$ as the average probability causing the robot to be repaired while passing a speed-control hump, then the total influence $c_{b_ h}$ caused by speed-

control humps in P_m is

$$c_{b_h} = P_{mh}r_{b_h} \quad (24)$$

With (21), (23) and (24), we obtain the cost c_b of P_m :

$$c_b = c_{b_r} + c_{b_h} = \frac{r_{b_h}}{\mu_f} \eta P_{mr} P_{ml} + P_{mh}r_{b_h} \quad (25)$$

4.2.3 Computing the Idle Time

The final purpose of various kinds of planners or optimizations is to maximize the working time. However, in this paper, we minimize the idle time (noted as T_{IDLE}) including recharging time T_C and repairing time T_R to achieve this purpose indirectly.

Define T_C (unit: s) as the time spent on recharging to compensate the energy consumption c_e , then

$$T_C = \frac{c_e}{v_{charge}} \quad (26)$$

where v_{charge} (unit: V/s) is the charging speed that can be derived by

$$v_{charge} = \frac{V_{full} - V_{low}}{T_C} \quad (27)$$

where V_{low} and V_{full} are the initial voltage value and the eventual value after fully charged respectively. In practice, v_{charge} can be measured experimentally.

In engineering, the Mean Time To Repair ($MTTR$) is usually used to describe the resumption performance of production. Here, we describe the cost c_b using $MTTR$. Let T_{MTTR} represent the $MTTR$ of our robot and note T_R (unit: s) as the repairing time induced by c_b then we have

$$T_R = c_b T_{MTTR} \quad (28)$$

Then T_{IDLE} is the sum of T_C and T_R , namely,

$$T_{IDLE} = T_C + T_R = \frac{c_e}{v_{charge}} + c_b T_{MTTR} \quad (29)$$

Since c_e and c_b are two elements of C , so, if we use function $f(C)$ to describe the relation between T_{IDLE} and C , i.e.,

$$T_{IDLE} = f(C) = f(c_e, c_b) = \frac{c_e}{v_{charge}} + c_b T_{MTTR} \quad (30)$$

4.3 Determining the Optimal Return-path

Based on the mathematical model of c_e , c_b and T_{IDLE} , the details of the procedure of determining the optimal return-path are described:

Step 1: Find out all the accessible paths to dock D_0 from the current position where the robot begins to return. Calculate the cost and idle time for each return-path and figure out the optimal return-path to dock D_0 .

Assume that there has N different return-paths accessible to dock D_0 , which are noted as $R_{D_0 0}$, $R_{D_0 1}$, ..., $R_{D_0 n}$, ..., $R_{D_0 (N-1)}$, and the costs are $C_{R_{D_0 0}}$, $C_{R_{D_0 1}}$, ..., $C_{R_{D_0 n}}$, ..., $C_{R_{D_0 (N-1)}}$ respectively. Note that each return-path is constituted by a sequence of segments. As an example, for a certain $R_{D_0 n}$ ($n=0,1,...,N-1$), assume that it is constituted by G ($0 < G \leq M$) segments and the order is $P_0, P_1, ..., P_g, ..., P_{G-1}$, then we express $R_{D_0 n}$ as

$$R_{D_0 n} = \{P_0, P_1, ..., P_g, ..., P_{G-1}\} \quad (31)$$

For a segment P_g ($g=0,1,...,G-1$), we note its cost as

$$C_{P_g} = (c_{e_P_g}, c_{b_P_g}) \quad (32)$$

Thus, $C_{R_{D_0 n}}$ ($n=0,1,...,N-1$) is the sum of C_{P_g} :

$$C_{R_{D_0 n}} = (c_{e_R_{D_0 n}}, c_{b_R_{D_0 n}}) = \left(\sum_{g=0}^{G-1} c_{e_P_g}, \sum_{g=0}^{G-1} c_{b_P_g} \right) \quad (33)$$

We use $T_{IDLE_R_{D_0 n}}$ to describe the idle time caused by $R_{D_0 n}$, then according to (30) and (33), we have

$$T_{IDLE_R_{D_0 n}} = f(C_{R_{D_0 n}}) = f\left(\sum_{g=0}^{G-1} c_{e_P_g}, \sum_{g=0}^{G-1} c_{b_P_g}\right) \quad (34)$$

After computing the idle for each return-path $R_{D_0 n}$, we select out the optimal one and note it as R_{D_0} . The criterion of selection is

$$T_{IDLE_R_{D_0}} = \min\{T_{IDLE_R_{D_0 n}} | n=0,1,...,N-1\} \quad (35)$$

where the decision function \min that will appear in (36) and (37) again means selecting the one with minimum value.

Step2: Figure out the respective optimal return-path to each dock D_h ($h=0,1,...,H-1$).

After performing the same process for the h 'th ($h=0,1,\dots,H-1$) dock, $H-1$ optimal return-paths to the other docks are derived, which are marked as $R_{D_1}, R_{D_2}, \dots, R_{D_h}, \dots, R_{D_{H-1}}$. For each R_{D_h} ($h=0,1,\dots,H-1$), we have

$$T_{IDLE_R_{D_h}} = \min\{T_{IDLE_R_{D_hn}} \mid n=0,1,\dots,N-1\} \quad (36)$$

Setp 3: From $R_{D_0}, R_{D_1}, \dots, R_{D_h}, \dots, R_{D_{H-1}}$, we determine the optimal return-path, and note it as $R_{D_{OP}}$. This optimal return-path is what we want finally, and is selected by

$$T_{IDLE_R_{OP}} = \min\{T_{IDLE_R_{D_h}} \mid h=0,1,\dots,H-1\} \quad (37)$$

5. Simulation, Results and Discussions

This section will first determine the values of parameters by experiments, then the simulation, results and discussions will be presented.

5.1. Determination of the Values of Parameters Experimentally

Here we will compute the values of relevant parameters appeared in Sect. 3 and Sect. 4 through experiments.

(a). $r_{e_μ_f}$ and $r_{e_μ_f φ_g}$.

First, we measure the values of $r_{e_μ_f}$ and $r_{e_μ_f φ_g}$ appeared in (18) in Sect. 4.2 in order to compute r_e .

Assume that V_{start} is the voltage value when the robot begins to work, and V_{end} the value after running at the average speed \bar{v} for time \bar{t} , then r_e (unit: V/m) is calculated as

$$r_e = \frac{V_{start} - V_{end}}{v\bar{t}} \quad (38)$$

Actually, some researches have tried to classify the terrain based on vibrations induced by wheel-terrain interaction [24]. Similarly, in this paper, observed from the real environment, the road surfaces are divided into two kinds, i.e., the flat surface and the rough surface, which are shown in Fig. 1(a) and Fig. 1(b) respectively. We use $μ_f$ and $μ_r$ to describe the surface roughness of these two typical roads respectively. The energy consumption rates $r_{e_μ_f}$ and $r_{e_μ_f φ_g}$ are estimated in the following.

A Pioneer3-AT robot produced by MobileRobot Inc. is utilized in the experiment [28]. Three lead acid cells are employed to provide energy for the robot, and the full voltage V_{full} is observed to be $12.7V$. In practice, to

ensure that the robot has enough power to go to the nearest dock wherever it begins to return, the threshold voltage V_{low} warning the robot to return for recharging is set to be $11.3V$. In the experiments, the robot starts to run at full voltage, and keeps running at the average speed of $\bar{v}=0.75m/s$ till the voltage valve decreases to $11.3V$. After testing many times on flat road of roughness $μ_f$, the average continuous running time \bar{t}_f is measured to be about 2.67 hours. Hence, $r_{e_μ_f}$ is derived:

$$r_{e_μ_f} = \frac{12.7V - 11.3V}{0.75m/s \times 2.67h \times 3600s/h} \approx 0.1942 \times 10^{-3} V/m \quad (39)$$

The same tests are repeated on a rough road of roughness $μ_r$, and we get $\bar{t}_r \approx 2.07h$, therefore,

$$r_{e_μ_r} = \frac{12.7V - 11.3V}{0.75m/s \times 2.07h \times 3600s/h} \approx 0.2505 \times 10^{-3} V/m \quad (40)$$

Actually, according to (15), $r_{e_μ_r} = \frac{μ_r}{μ_f} r_{e_μ_f}$, Therefore,

with (39) and (40), the relation between $μ_f$ and $μ_r$ is derived:

$$μ_r = \frac{r_{e_μ_r}}{r_{e_μ_f}} μ_f = \frac{0.2505 \times 10^{-3}}{0.1942 \times 10^{-3}} μ_f \approx 1.2899 μ_f \quad (41)$$

In addition, we do the similar experiments on a slope of surface roughness $μ_f$, road grade $φ_g \approx 0.087rad$ and length $L=100m$. The robot is running uphill with the average speed of $\bar{v}=0.75m/s$. After testing several times, we get the mean value of $r_{e_μ_f φ_g}$:

$$r_{e_μ_f φ_g} \approx 0.2034 \times 10^{-3} V/m \quad (42)$$

(b). $r_{b_μ_f}$ and r_{b_h} .

The experiment carried out on the flat road of surface roughness $μ_f$ announces that, at the average speed of $\bar{v}=0.75m/s$, the robot needs to be repaired after four weeks continuous working of five hours a day and seven days a week. According to (22), $r_{b_μ_f}$ is

$$r_{b_μ_f} = \frac{1}{7 \times 4 \times 5h \times 0.75m/s \times 3600s/h} \approx 0.2646 \times 10^{-5} m^{-1} \quad (43)$$

Another test on a path of surface roughness $μ_r$, and the days are measured to be 13, so $r_{b_μ_r}$ is

$$r_{b_μ_r} = \frac{1}{13 \times 5h \times 0.75m/s \times 3600s/h} \approx 0.5698 \times 10^{-5} m^{-1} \quad (44)$$

With (41), (43) and (44), the parameter η in (23) is calculated as

$$\eta = \frac{r_{b_h} \mu_r \mu_f}{r_{b_h} \mu_r \mu_f} = \frac{0.5698 \times 10^{-5}}{0.2645 \times 10^{-5} \times 1.2899} \approx 1.6701 \quad (45)$$

For r_{b_h} , if tested that the robot has to be maintained after passing a speed-control hump for Γ times successively, then

$$r_{b_h} = \frac{1}{\Gamma} \quad (46)$$

The experiment is implemented on flat road where a speed-control hump is placed. The robot passes the speed-control hump back and forth at the average speed of $\bar{v} = 0.75m/s$. The result is $\Gamma \approx 1300$, thus

$$r_{b_h} = \frac{1}{1300} \approx 0.7692 \times 10^{-3} \quad (47)$$

(c). v_{charge} and T_{MTTR} .

In experiment, it will take about 2.5 hours for charging from 11.3V to 12.7V for the Pioneer3-AT robot, i.e., $T_C = 2.5h$. With (27), we obtain the charge speed

$$v_{charge} = \frac{13.7V - 11.3V}{2.5h \times 3600s/h} \approx 0.1556 \times 10^{-3} V/s \quad (48)$$

In addition, the time spent on repairing our robot is 4 hours once on average, hence, T_{MTTR} appeared in (28) is

$$T_{MTTR} = 4h \times 3600s/h = 1.44 \times 10^4 s \quad (49)$$

5.2. Results and Discussions

The topological map (noted as C_i) shown in Fig. 5 is built in accordance with the real environment. In addition, the attributes of the multiple road segments are gathered in Table 1.

In C_i , the robot is at the point S_R where the power is checked lower than the threshold voltage. As there are three docks, we first find out all the accessible return-paths to docks D_0, D_1 and D_2 , and calculate the cost to each dock respectively. Then we select the respective optimal return-path to each dock by applying the strategy proposed. The constitution of each return-path, the total path length (L_T for short), the cost and idle time are listed out in Table 2. Finally, the final optimal one is derived by comparing the idle time of each return-path.

Note that in Table 1, there are 24 segments existing in the working environment. In additional, $P_{S_R O}$ represents the segment from point S_R to point O , and $P_{S_R P}$ is the segment from S_R to P .

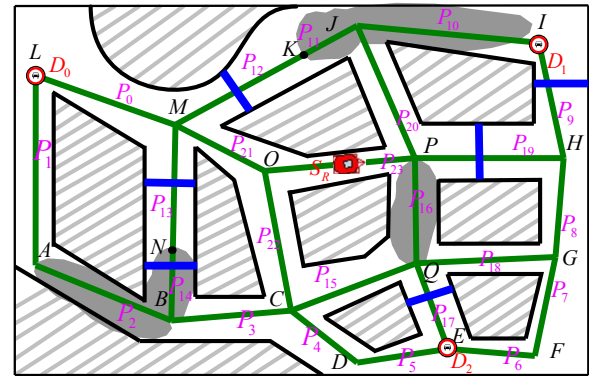


Figure 5. The topological map built based on the real working environment.

P_m	$(p_{ml}, p_{mr}, p_{mg}, p_{mh})$	P_m	$(p_{ml}, p_{mr}, p_{mg}, p_{mh})$
P_0	$(119.6, \mu_f, 0, 0)$	P_1	$(155.0, \mu_f, 0.05, 0)$
P_2	$(119.0, \mu_r, 0, 0)$	P_3	$(97.5, \mu_f, 0, 0)$
P_4	$(71.0, \mu_f, 0.18, 0)$	P_5	$(75.3, \mu_f, 0, 0)$
P_6	$(75.3, \mu_f, 0, 0)$	P_7	$(84.2, \mu_f, 0.12, 0)$
P_8	$(83.0, \mu_f, 0, 0)$	P_9	$(96.9, \mu_f, -0.06, 0.1)$
P_{10}	$(150.7, \mu_r, -0.09, 0)$	P_{11}	$(48.8, \mu_r, 0.52, 0)$
P_{12}	$(117.4, \mu_f, 0.21, 1)$	P_{13}	$(102.0, \mu_f, 0.08, 1)$
P_{14}	$(53.2, \mu_r, 0.21, 1)$	P_{15}	$(101.9, \mu_f, 0.16, 0)$
P_{16}	$(100.2, \mu_r, 0, 0)$	P_{17}	$(84.2, \mu_f, 0, 1)$
P_{18}	$(124.1, \mu_f, 0, 0)$	P_{19}	$(124.0, \mu_f, 0, 1)$
P_{20}	$(115.2, \mu_f, 0, 0)$	P_{21}	$(84.6, \mu_f, -0.09, 0)$
P_{22}	$(116.0, \mu_f, -0.07, 0)$	P_{23}	$(119.0, \mu_f, -0.08, 0)$
$P_{S_R O}$	$(57.0, \mu_f, -0.08, 0)$	$P_{S_R P}$	$(62.0, \mu_f, -0.08, 0)$

Table 1. The attributes of each segment in map C_i .

According to the map C_i , 39 different accessible return-paths to dock D_0 can be found, among which the optimal one $R_{D_0} = \{P_{S_R O}, P_{21}, P_0\}$ is picked out. As listed in Table 2, the cost $C_{R_{D_0}}$ is $(0.0520, 1.1543 \times 10^{-3})$ and the idle time $T_{IDLE_R_{D_0}}$ is 350.897s. The optimal return-paths to docks D_1 and D_2 are also shown in Table 2, with the respective cost and idle time. Observed from Table 2, if the decision factor was path length, the optimal return-path would be R_{D_2} which has the shortest length 246.4m. However, this path will cause more idle time than R_{D_0} practically, the extra idle time is

$$\Delta T_{IDLE} = 368.496s - 350.897s = 17.599s \quad (50)$$

The comparison shows that the strategy proposed in this paper is more effective than the traditional ones taking the path length as the decision factor.

D_h	D_0	D_1	D_2
R_{D_h}	$\{P_{SRO}, P_{21}, P_0\}$	$\{P_{SRP}, P_{19}, P_9\}$	$\{P_{SRP}, P_{16}, P_{17}\}$
L_T / m	262.1	282.9	246.4
(c_e, c_b)	(0.0520, 1.1543×10^{-3})	(0.0543, 2.7886×10^{-3})	(0.0529, 1.9864×10^{-3})
T_{IDLE} / s	350.897	389.347	368.496

Table 2. The optimal return-path to each dock D_h ($h=0,1,2$) as well as the constitution of each R_{D_h} ($h=0,1,2$), the total path length L_T , the cost and the idle time.

The application of this strategy will have notable effect in the long run rather than judged by a single returning process. Statistically, if the robot returns to recharge four times a day on average and $\Delta T_{IDLE} = 17.599s$ is taken as an example, the total idle time T_{SAVE} (unit: hour) being saved in a year (given 360 days) owing to the implementation of this strategy is calculated as

$$T_{SAVE} = \frac{17.599s \times 4 \times 360}{3600s/h} = 7.04h \quad (51)$$

Given $T_{MTTR} = 4h$, this value shows that the robot can be absent from maintaining N times in a year, and

$$N = \frac{T_{SAVE}}{T_{MTTR}} = \frac{7.04h}{4h} = 1.76 \quad (52)$$

The saved idle time, or the time of missing operation due to maintenance, manifests the important significance in practice.

6. Conclusion and Future Work

We have proposed a strategy of optimal return-path determination for mobile robot recharging in outdoor environment in consideration of road attributes, and described the decision mechanism afterwards. The strategy is implemented and compared with the traditional method in simulation. The results verify the effectiveness and show the superiority of our strategy, and the practical significance has been clarified by the reported analysis. In a future work, the taking into account of the stochasticity of parameter values will be introduced in order to make the model more suitable for real case. We will apply this strategy on our patrol robot that works in a transformer substation.

7. Acknowledgements

This research was sponsored by project No. CDJXS11171158 supported by the Fundamental Research Funds for the Central Universities and the Key Project of Science and Technology Committee of Chongqing (CSTC,

2009AB2139). The authors are also thankful to the anonymous reviewers for their comments and suggestions.

8. References

- [1] K. Z. Wang, S. Liang, H. B. Bi, and X. D. Xian, "Implementation of a robot inspection system for substation equipment based on pioneer 3-AT," ICIC Express Letters, Part B: Applications, vol. 2, no. 1, pp. 221–226, 2011.
- [2] T. Kesavadas, "Automated guided vehicles/self guided vehicles." UB, North Campus, 2007. [Online]. Available: <http://wings.buffalo.edu/eng/mae/courses/460-564/AGV.pdf>.
- [3] A. Chella and I. Macaluso, "The perception loop in cicerobot, a museum guide robot," Neurocomputing, vol. 72, no. 4-6, pp. 760–766, 2009.
- [4] Y. G. Mei, Y. H. Lu, Y. C. Hu, and C. S. G. Lee, "Deployment of mobile robots with energy and timing constraints," IEEE Transactions on robotics, vol. 22, no. 3, pp. 507–522, 2006.
- [5] M. C. Silverman, D. Nies, B. Jung, and G. S. Sukhatme, "Staying alive: A docking station for autonomous robot recharging," in IEEE International Conference on Robotics and Automation, (Washington, D. C.), pp. 1050–1055, 2002.
- [6] R. Aylett, Robots: Bringing Intelligent Machines to Life. Barron's Educational Series, 1 ed., 2002.
- [7] J. Wawerla and R. T. Vaughan, "Near-optimal mobile robot recharging with the rate-maximizing forager," in In European Conference on Artificial Life, (Lisbon, Portugal), pp. 776–785, 2007.
- [8] A. F. Cook IV and C. Wenk, "Link distance and shortest path problems in the plane," Computational Geometry: Theory and Applications, vol. 44, pp. 442–455, 2011.
- [9] T. C. Liang, J. S. Liu, G. T. Hung, and Y. Z. Chang, "Practical and flexible path planning for car-like mobile robot using maximal-curvature cubic spiral," Robotics and Autonomous Systems, vol. 52, pp. 312–335, 2005.
- [10] H. Liu and J. Zhou, "Motion planning for human-robot interaction based on stereo vision and sift," in Proceedings of the 2009 IEEE International Conference on Systems, Man, and Cybernetics, (San Antonio, TX, USA), pp. 830–834, 2009.
- [11] K. L. Su, C. Y. Chung, Y. L. Liao, and J. H. Guo, "Searching algorithm based path planning of mobile robots," ICIC Express Letters, Part B: Applications, vol. 2, no. 1, pp. 273–278, 2011.
- [12] M. X. Yuan, S. A. Wang, C. Y. Wu, and C. N. Jian, "A novel immune network strategy for robot path planning in complicated environments," Journal of Intelligent & Robotic Systems, vol. 60, pp. 111–131, 2010.

- [13] Y. G. Mei, Y. H. Lu, C. S. G. Lee, and Y. C. Hu, "Energy-efficient mobile robot exploration," in *Proceedings of the 2006 IEEE International Conference on Robotics and Automation*, (Orlando, Florida), pp. 505–511, 2006.
- [14] Z. Sun and J. Reif, "On energy-minimizing paths on terrains for a mobile robot," in *IEEE International Conference on Robotics and Automation*, (Taipei, Taiwan), pp. 3782–3788, 2003.
- [15] L. Aleksandrov, A. Maheshwari, and J. R. Sack, "Determining approximate shortest paths on weighted polyhedral surfaces," *Journal of the ACM*, vol. 51, no. 1, pp. 25–53, 2005.
- [16] D. Z. Chen, O. Daescu, X. Hu, X. Wu, and J. Xu, "Determining an optimal penetration among weighted regions in two and three dimensions," *Journal of Combinatorial Optimization*, vol. 5, no. 1, pp. 59–79, 2001.
- [17] D. Gaw and A. Meystel, "Minimum-time navigation of an unmanned mobile robot in a 2-1/2d world with obstacles," in *Proc. 1986 IEEE International Conference on Robotics and Automation*, (San Francisco, CA), pp. 1670–1677, 1986.
- [18] Z. Sun and J. H. Reif, "On finding energy-minimizing paths on terrains," *IEEE Transactions on Robotics*, vol. 21, no. 1, pp. 102–114, 2005.
- [19] Z. Sun and J. H. Reif, "On finding approximate optimal paths in weighted regions," *Journal of Algorithms*, vol. 58, pp. 1–32, 2006.
- [20] P. L. E. J. D. Guo, Y. and Z. Y. Dong, "Performance-based rough terrain navigation for nonholonomic mobile robots," in *The 29th Annual Conference of the IEEE Industrial Electronics Society*, (Virginia, United States), pp. 2881–2886, 2003.
- [21] N. C. Rowe and R. S. Ross, "Optimal grid-free path planning across arbitrarily contoured terrain with anisotropic friction and gravity effects," *IEEE Transactions on Robotics and Automation*, vol. 6, no. 5, pp. 540–553, 1990.
- [22] M. Cherif, "Motion planning for all-terrain vehicles: A physical modeling approach for coping with dynamic and contact interaction constraints," *IEEE Transactions on Robotics and Automation*, vol. 15, no. 2, pp. 202–218, 1999.
- [23] M. B. Kobilarov and G. S. Sukhatme, "Near time-optimal constrained trajectory planning on outdoor terrain," in *Proceedings of the 2005 IEEE International Conference on Robotics and Automation*, (Barcelona, Spain), pp. 1833–1840, 2005.
- [24] C. Brooks, L. Karl, and S. Dubowsky, "Vibration-based terrain analysis for mobile robots," in *Proceedings of the 2005 IEEE International Conference on Robotics and Automation*, (Barcelona, Spain), pp. 3415–3420, 2005.
- [25] E. M. Dupont, C. A. Moore, and R. G. Roberts, "Terrain classification for mobile robots traveling at various speeds: An eigenspace manifold approach," in *IEEE International Conference on Robotics and Automation*, (Pasadena, CA, USA), pp. 3284–3289, 2008.
- [26] K. Bogsjö, K. Podgórski, and I. Rychlik, "Models for road surface roughness," tech. rep., Department of Mathematical Sciences, Division of Mathematical Statistics, Chalmers University of Technology and University of Gothenburg, 2010. [Online]. Available: <http://www.math.chalmers.se/Math/Research/Preprints/2010/42.pdf>.
- [27] P. Sahlholm and K. H. Johansson, "Road grade estimation for look-ahead vehicle control using multiple measurement runs," *Control Engineering Practice*, no. 18, pp. 1328–1341, 2010.
- [28] MobileRobot Inc., *Pioneer3 Operations Manual*, 2006. [Online]. Available: <http://www.ist.tugraz.at/attach/Publish/Kmr06/pioneer-robot.pdf>.

Corrigendum to *Determination of an Optimal Return-path on Road Attributes for Mobile Robot Recharging*

Fei Liu^{*1}, Shan Liang¹ and Xiaodong Xian¹

¹ College of Automation, Chongqing University, China

* Corresponding author E-mail: liufei2119@yahoo.com.cn

[Paper originally published 01 November, 2011](#)

DOI: 10.5772/55068

© 2012 Liu et al.; licensee InTech. This is an open access article distributed under the terms of the Creative Commons Attribution License (<http://creativecommons.org/licenses/by/3.0>), which permits unrestricted use, distribution, and reproduction in any medium, provided the original work is properly cited.

This corrigendum is offered as a means to correct errors in "Determination of an Optimal Return-path on Road Attributes for Mobile Robot Recharging" (Fei Liu, Shan Liang, Xiaodong Xian, *International Journal of Advanced Robotic Systems*, vol.8, no.5, pp. 83-92, 2011). The error is due to the fact that we reckoned without taking into account the energy consumed by the sensors on the robot. Please see the corrections below.

Page 85-86

(1) In column 2, the last paragraph should read:

(c) The cost that the robot will pay for passing each segment includes two parts: energy consumption c_e and the influence of vibration on the robot body c_b that describes the probability of the robot's equipment failure. **Actually, c_e includes two parts, the part that the sensors on the robot will consume, and secondly, the energy used for driving the motor. Here, we use c_s to describe the first part and use \hat{c}_e to describe the second part. Therefore,**

$$c_e = \hat{c}_e + c_s \quad (1)$$

Then the cost C can be described as

$$C = (c_e, c_b) \quad (2)$$

Page 86

(1) In column 2, the chapter title "4.2.1 Mathematical Model of c_e " should read: "4.2.1 Mathematical Model of \hat{c}_e ".

(2) In column 2, the paragraphs after equation (9) and before equation (11), all c_e should be replaced by \hat{c}_e .

(3) In column 2, equation (10) should be

$$\hat{c}_e = \lambda W_{p_{ml}} \quad (3)$$

(4) In column 2, equation (11) should be

$$\hat{c}_e = r_e p_{ml} \quad (4)$$

Page 87

(1) In column 2, equation (20) should be

$$\hat{c}_e = (\Delta r_{e_r} p_{mr} \cos(p_{mg}) + \Delta r_{e_g} \sin(p_{mg})) p_{ml} \quad (5)$$

Page 88

(1) In column 1, after equation (25) in chapter 4.2.2, the following should be added:

4.2.3 Mathematical Model of c_s

First, we define r_s as the energy consumption rate, which describes how much energy the sensor will consume when the robot walks for a unit distance. The value of r_s is always stable, so for any road segment, for passing distance p_{ml} , we have the energy consumption

$$c_s = r_s p_{ml} \quad (6)$$

(2) In column 2, chapter title “4.2.3 Computing the Idle Time” should be replaced by “4.2.4 Computing the Idle Time”.

Page 89

(1) In column 1, after the first paragraph in chapter 5.1, the following should be added:

$$(a) \quad r_s$$

Here, we do not measure r_s directly, on the contrary, we first measure the consumption rate for unit time, which can be termed τ_s (unit: V/s). If V_{start} (unit: V) is the voltage value when the robot is just powered on, and after a period of time t , the value decreases to V_{end} (unit: V), we get

$$\tau_s = \frac{V_{start} - V_{end}}{t} \quad (7)$$

We assume that the robot walking for distance p_{ml} at average speed \bar{v} (unit: m/s), then

$$r_s = \frac{\tau_s}{\bar{v}} \quad (8)$$

In our experiment, we set $V_{start} = 12.7V$, $V_{end} = 11.3V$, $\bar{v} = 0.75m/s$, then it is measured that $t = 4.5h$,

therefore, r_s is measure to be

$$r_s = \frac{12.7V - 11.3V}{0.75m/s \times 4.5h \times 3600s/h} \approx 0.1152V/m \quad (9)$$

(2) Equation (38) should be

$$r_e = \frac{V_{start} - V_{end}}{vt} - r_s \quad (10)$$

(3) Equation (39) should be

$$r_{e-\mu_f} = \frac{12.7V - 11.3V}{0.75m/s \times 2.67h \times 3600s/h} - 0.1152 \times 10^{-3} V/m \quad (11)$$

$$\approx 0.0790 \times 10^{-3} V/m$$

(4) Equation (40) should be

$$r_{e-\mu_r} = \frac{12.7V - 11.3V}{0.75m/s \times 2.07h \times 3600s/h} - 0.1152 \times 10^{-3} V/m \quad (12)$$

$$\approx 0.1353 \times 10^{-3} V/m$$

(5) Equation (41) should be

$$\mu_r = \frac{r_{e-\mu_r}}{r_{e-\mu_f}} \mu_f = \frac{0.1353 \times 10^{-3}}{0.0790 \times 10^{-3}} \mu_f \approx 1.7127 \mu_f \quad (13)$$

(6) Equation (42) should be

$$r_{e-\mu_f \phi_g} \approx 0.2034 \times 10^{-3} V/m - 0.1152 \times 10^{-3} V/m \quad (14)$$

$$= 0.0882 \times 10^{-3} V/m$$

Page 90

(1) Equation (45) should be

$$\eta = \frac{r_{b-\mu_r} \mu_f}{r_{b-\mu_f} \mu_r} = \frac{0.5698 \times 10^{-5}}{0.2645 \times 10^{-5} \times 1.7127} \approx 1.2578 \quad (15)$$

(2) In the penultimate paragraph of column 2, the following corrections should be made:

As listed in Table 2, the cost $C_{R_{D_0n}}$ is $(0.0520, 0.8693 \times 10^{-3})$ and the idle time $T_{IDLE_R_{D_0}}$ is $346.834s$.

(3) Equation (50) should be

$$\Delta T_{IDLE} = 366.547s - 346.834s = 19.713s \quad (16)$$

(1) Table 2 should be replaced by

D_h	D_0	D_1	D_2
R_{D_h}	$\{P_{S_{RO}}, P_{21}, P_0\}$	$\{P_{S_{RP}}, P_{19}, P_9\}$	$\{P_{S_{RP}}, P_{16}, P_{17}\}$
L_T / m	262.1	282.9	246.4
(c_e, c_b)	(0.0520, 0.8693×10^{-3})	(0.0544, 2.4780×10^{-3})	(0.0529, 1.1827×10^{-3})
T_{IDLE} / s	351.361	390.160	372.055

Table 2. The optimal return-path to each dock $D_h (h=0,1,2)$ as well as the constitution of each $R_{D_h} (h=0,1,2)$, the total path length L_T , the cost and the idle time.

(2) In column 2, in the paragraph below table 2, the following corrections should be made:

Statistically, if the robot returns to recharge four times a day on average and $\Delta T_{IDLE} = 20.694s$ is taken as an example,

(3) Equation (51) should be

$$T_{SAVE} = \frac{19.71s \times 4 \times 360}{3600s/h} = 7.88h \quad (17)$$

(4) Equation (52) should be

$$N = \frac{T_{SAVE}}{T_{MTTR}} = \frac{7.88h}{4h} = 1.97 \quad (18)$$